

PAPER

# Analytical model for memristive systems for neuromorphic computation

To cite this article: Sanjay Kumar *et al* 2021 *J. Phys. D: Appl. Phys.* **54** 355101

View the [article online](#) for updates and enhancements.

## You may also like

- [Y<sub>2</sub>O<sub>3</sub>-based memristive crossbar array for synaptic learning](#)  
Mohit Kumar Gautam, Sanjay Kumar and Shaibal Mukherjee
- [Dynamic resistive switching devices for neuromorphic computing](#)  
Yuting Wu, Xinxin Wang and Wei D Lu
- [An enhanced lumped element electrical model of a double barrier memristive device](#)  
Enver Solan, Sven Dirkmann, Mirko Hansen *et al.*



The Electrochemical Society  
Advancing solid state & electrochemical science & technology

242nd ECS Meeting

Oct 9 – 13, 2022 • Atlanta, GA, US

Abstract submission deadline: **April 8, 2022**

Connect. Engage. Champion. Empower. Accelerate.

**MOVE SCIENCE FORWARD**



Submit your abstract



# Analytical model for memristive systems for neuromorphic computation

Sanjay Kumar<sup>1</sup>, Rajan Agrawal<sup>1</sup>, Mangal Das<sup>3</sup> , Kumari Jyoti<sup>1</sup>, Pawan Kumar<sup>1</sup> and Shaibal Mukherjee<sup>1,2,\*</sup> 

<sup>1</sup> Hybrid Nanodevice Research Group (HNRG), Electrical Engineering, Indian Institute of Technology Indore, Indore, Madhya Pradesh 453552, India

<sup>2</sup> Centre for Advanced Electronics (CAE), Indian Institute of Technology Indore, Indore, Madhya Pradesh 453552, India

<sup>3</sup> Electrical Engineering, Indian Institute of Technology, Bombay, Powai, Mumbai 400076, India

E-mail: [shaibal@iiti.ac.in](mailto:shaibal@iiti.ac.in)

Received 17 April 2021

Accepted for publication 3 June 2021

Published 17 June 2021



## Abstract

From the last decade, the development of a generic model for memristive systems which simulates the biologically inspired nervous system of living beings, is one of the most attracting aspects. More specifically, the develop generic model has capability to resolve the problems in the field of artificial neural network. Here, a generic, non-linear analytical memristive model, which is based on interfacial switching mechanism, has been discussed. The proposed model has the capability to simulate the high-density neural network of biological synapses that regulates the communication efficacy among neurons and can implement the learning capability of the neurons. Further, the proposed model is the parallel connection of the rectifier and memristor which shows better non-linear profile along with non-ideal effects and rectifying nature in its pinched hysteresis loop in the resistive switching characteristics. Moreover, proposed model shows the significant low value of maximum error deviation  $\sim 4.44\%$  for  $\text{Y}_2\text{O}_3$ -based and  $\sim 4.5\%$  for  $\text{WO}_3$ -based memristive systems, respectively in its neuromorphic characteristics with respect to the corresponding experimental results. Therefore, the proposed analytical memristive model can be utilized to develop the memristive system for real-world applications based on neuromorphic behaviors of any transition metal oxide-based memristive systems.

Keywords: artificial neuron, modeling, neuromorphic computation, memristive systems

(Some figures may appear in color only in the online journal)

## 1. Introduction

Artificial brain-inspired computing is a growing domain of research and it can extend the capabilities of information technology beyond the Von Neumann architecture [1]. Generally, biologically inspired nervous systems, which aim to emulate the biological nervous system, are the perfect solutions to resolve the problems such as development of artificial neural network [2], analogue signal [3] and image processing [3]. In the biological nervous systems, neurons are inter-connected through synapses [4, 5], where synaptic weight is analogues

to normalized device conductance which can be varied under the influence of an electrical stimuli [5]. The synaptic weight is debilitated and strengthened under the excitation of negative and positive electrical signal, respectively [4] and these mechanisms are known as depression and potentiation, respectively.

In general, the plasticity is the functionality of the brain to change and adapt to new information. Similarly, synaptic plasticity is the temporary change in the synapse between two neurons which allow neurons to communicate to each other and transfer the information from pre- to post-synapse [6]. The strength of communication between two neurons can be dependent on synapses which further, linked to other neurons for volumetric conversation. The volumetric conversation of the synapse is not static, but rather can change in both

\* Author to whom any correspondence should be addressed.

the short-term and long-term modes [6]. Synaptic plasticity refers to these changes in synaptic strength. The ability of change in synaptic weight is called synaptic plasticity and it is a key mechanism pursued by the human brain in learning process [7]. Artificial neural networks, which are inspired by the remarkable efficiency of biological systems, can be practically realized by the memristive system [8]. The neuromorphic application requires low-power, high-density, and complementary-metal oxide semiconductor (CMOS) compatible devices and systems [8]. All these features are offered by memristive systems, making them highly suitable for neuromorphic computation [5], synaptic functionality [9], and data storage applications [10]. In a neuromorphic computational system, memristor will act as synapse and biological neuron blocks are built by using CMOS processes which are having high versatility for the neuromorphic system.

Several experimental reports in the literature based on various material systems such as  $\text{WO}_3$  [4],  $\text{TiO}_2$  [11],  $\text{HfO}_2$  [7] and  $\text{ZnO}$  [12] show synaptic functionality which is comparable to biological synapse. Recently, our group has successfully demonstrated the  $\text{Y}_2\text{O}_3$ -based [13–16] memristive system for neuromorphic applications in which the dielectric layer (yttria,  $\text{Y}_2\text{O}_3$ ) is grown by using dual ion beam sputtering (DIBS) system. DIBS system offers various advantages such as high-quality thin films with better compositional stoichiometry, small surface roughness and good adhesion of film to the substrate [13, 14] compared to other conventional physical vapor deposition techniques. The above-mentioned memristive systems have shown non-linear asymmetric behavior in the resistive switching characteristics. Published literatures have reported models based on analytical [17, 18] and SPICE circuit simulation [4, 19] exhibit large error margin while matching with the corresponding experimental data. In fact, some of these models [18, 19] have not even been validated with any experimental reports at all. However, till date, to the best of authors' knowledge, a detailed non-linear analytical memristive model is unavailable which could be matched with experimental characteristics of various memristive systems which are based on interfacial switching mechanism such as the memristive systems based on  $\text{Y}_2\text{O}_3$  and  $\text{WO}_3$  materials and to analyze the performance of such systems.

In this article, a non-linear current–voltage ( $I$ – $V$ ) relationship along with a new piecewise window function has been proposed to study and analyze the performance of the memristive system. Recently, Kumar *et al* [20] have reported a semi-empirical model to remove the inconsistencies in lack of non-linear profile in the drift current at device boundaries. However, that model does not capture the physics of a memristive system which is based on the interfacial switching mechanism. The maximum error deviation (MED) of the reported model [20] has been  $\sim 20.2\%$ , which is larger than the current proposed non-linear model. The proposed non-linear analytical model is the parallel connection of rectifier and memristor, as shown an inset of figure 1, which covers a better non-linear profile along with non-ideal effects of the switching characteristics such as asymmetrical and non-zero crossing nature of switching and rectifying nature in the resistive switching characteristics. The proposed non-linear

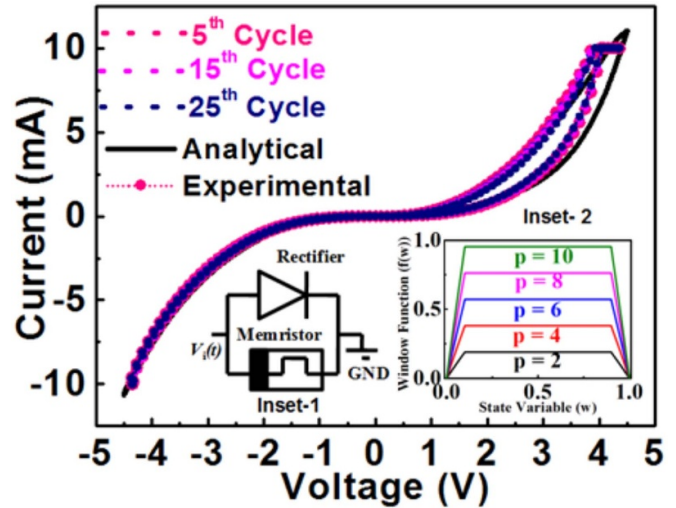


**Figure 1.** Resistive switching characteristic of a memristive device (sweep rate:  $1.042 \text{ V s}^{-1}$ ). Inset-1 and inset-2 show parallel connection of rectifier and memristor and piecewise window function, respectively.

analytical model is validated with the help of experimental results on  $\text{Y}_2\text{O}_3$  [13] and  $\text{WO}_3$  [4] (see appendix) based memristive systems and the modeled data shows  $\sim 4.44\%$  MED with the corresponding experimental results [13] and newly piecewise window function satisfies all the necessary conditions as reported by Prodromakis *et al* [21]. This work describes the detailed non-linear analytical model along with synaptic learning behavior and synaptic plasticity functionality of  $\text{Y}_2\text{O}_3$  and  $\text{WO}_3$ -based memristive systems.

## 2. Proposed analytical model

$I$ – $V$  relationship for the proposed non-linear analytical model is governed by the equation (1) which is closely related to the model equation reported by Yang *et al* [22]:

$$I(t) = \begin{cases} b_1 w^{a_1} (e^{\alpha_1 V_i(t)} - 1) + \chi (e^{\gamma V_i(t)} - 1), & V_i(t) \geq 0 \\ b_2 w^{a_2} (e^{\alpha_2 V_i(t)} - 1) + \chi (e^{\gamma V_i(t)} - 1), & V_i(t) < 0 \end{cases} \quad (1)$$

here, the first term on the right-hand side of equation (1) describes the flux-controlled memristive behavior and it is dominated by the interfacial switching mechanism which is not incorporated by various previously reported models [20, 22, 23]. The newly introduced parameters  $a_1$  and  $a_2$  are the degrees of influence of the state variable on current for positive and negative voltage biases, respectively.  $b_1$  and  $b_2$  are the experimental fitting parameters which define the slope of conductivity in  $I$ – $V$  characteristics,  $w$  is the state variable,  $\alpha_1$  and  $\alpha_2$  are the hysteresis loop area controlling parameters. The second term on the right-hand side of equation (1) is associated with the ideal diode behavior in  $I$ – $V$  characteristics which plays a vital role when the state variable ( $w$ ) approaches zero, i.e. the switching device is near to the OFF state and parameters  $\chi$  and  $\gamma$  denote the net electronic barrier of the memristive

device.  $V_i(t)$  is the applied input voltage and in the case of  $I$ - $V$  characteristics, a triangular waveform and while in the case of synaptic functionality, rectangular voltage pulses are used.

The proposed analytical model is applicable for both unipolar and bipolar memristive systems while previously reported models [21, 22] are utilized only for bipolar memristive system. Generally, due to higher conductivity under the positive bias condition, memristive devices show a larger hysteresis loop area, as shown in figure 1, as compared to that under the negative bias [4, 13]. This is due to the fact that under the application of positive bias, oxygen vacancies move towards the interface between Al used as the top electrode and  $Y_2O_3$  as switching oxide layer in the case for  $Y_2O_3$ -based memristive system [13]. The movements of these oxygen vacancies play a significant role in resistive switching phenomena at the Al/ $Y_2O_3$  interface. Moreover, Chang *et al* [4] also have experimentally reported similar resistive switching phenomena for  $WO_3$ -based memristive system at the Pt/ $WO_3$  interface. A new piecewise window function,  $f(w)$  is described by equation (2), as shown in the inset of figure 1, which ensures that the state variable ( $w$ ) is limited between 0 and 1. In the analytical modeling, a constant value of  $p = 2$  is used. The range of parameter  $p$  defines the limit of the  $f(w) \in \{0, 1\}$  (see inset-2 in figure 1) and if the value of  $p > 10$ , the upper limit of the  $f(w)$  is beyond 1 thus violating the essential conditions reported by Prodromakis *et al* [21]:

$$f(w) = \log \left\{ \begin{array}{ll} (1+w)^p, & 0 \leq w \leq 0.1 \\ (1.1)^p, & 0.1 < w \leq 0.9 \\ (2-w)^p, & 0.9 < w \leq 1 \end{array} \right\}. \quad (2)$$

The time derivative of the state variable ( $w(t)$ ) is governed by the equation (3) in which it depends on the nature of input voltage and window function:

$$\frac{dw}{dt} = A \times V_i^m(t) \times f(w) \quad (3)$$

where,  $A$  and  $m$  are the parameters that determine the dependence of the state variable on the input voltage and  $m$  is always an odd integer to ensure that the opposite polarity of the applied voltage leads to opposite change in the rate of change of state variable. Table 1 presents the physical significance and numerical values of all parameters used in analytical modeling.

### 3. Results and discussion

To investigate the various experimentally-obtained characteristics of  $Y_2O_3$ -based memristive system, similar electrical conditions are used which have been reported elsewhere [13]. To analyze the resistive switching characteristics, a chain of triangular voltage waveform is imposed on the device with peak-to-peak voltage of  $\pm 5$  V with a compliance current of 10 mA. Figure 1 shows the pinched hysteresis loop in resistive switching characteristics of developed memristive devices along with their modeled data. In order to calculate the MED of the modeled data with the corresponding experimental results,

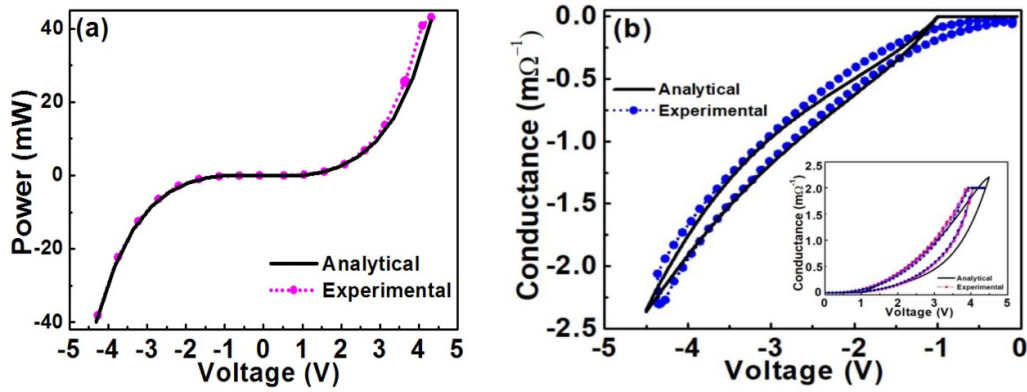
**Table 1.** Physical interpretation and values of parameters for analytical modeling.

Parameters	Values for $Y_2O_3$	Values for $WO_3$	Physical significance
$b_1$	$1.59 \times 10^{-3}$	$1.2 \times 10^{-5}$	Experimental fitting parameters
$b_2$	$-6.2 \times 10^{-4}$	$6.7 \times 10^{-7}$	Experimental fitting parameters
$a_1$	1.2	1.5	Degrees of influence of the state variable under positive bias
$a_2$	0.3	1.9	Degrees of influence of the state variable under negative bias
$\alpha_1$	0.60	0.80	Hysteresis loop area controlling parameters under positive bias
$\alpha_2$	-0.68	-1.5	Hysteresis loop area controlling parameters under negative bias
$\chi$	$1 \times 10^{-11}$	$1 \times 10^{-10}$	Magnitude of ideal diode behavior
$\gamma$	1	1	Diode parameters like thermal voltage and ideality factor
$A$	$5 \times 10^{-4}$	$3 \times 10^{-4}$	Control the effect of the window function
$m$	5	5	Control the effect of input on the state variable
$p$	$0 < p \leq 10$ ; $p = 2$ (for result validation with the reported experimental data [13])	$0 < p \leq 10$ ; $p = 1.5$ (for result validation with the reported experimental data [4])	Bounding parameter for window function between 0 and 1

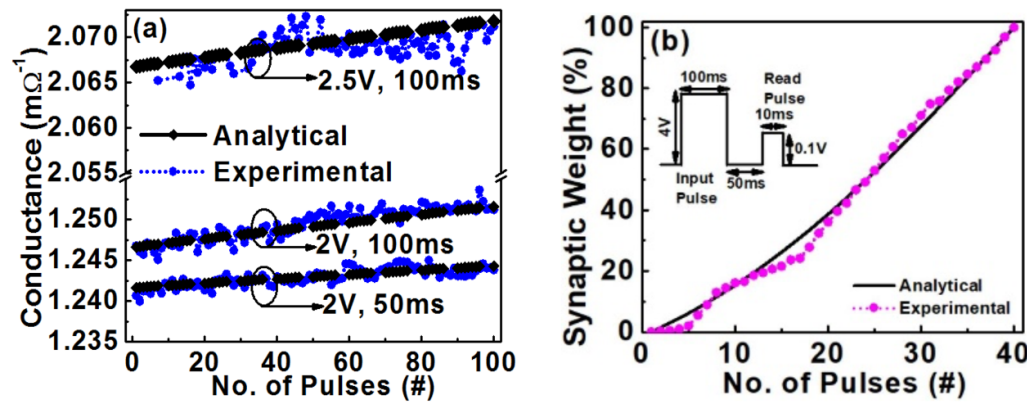
similar mathematical pathway is used which has been reported by Bakar *et al* [24], Hemmati *et al* [25], and Kumar *et al* [20]. By utilizing this formulation, the modeled data shows  $\sim 18.5\%$  MED at +4 V in  $I$ - $V$  characteristic as shown in figure 1 with respect to the experimental data of the developed device. The presence of a pinched hysteresis loop in resistive switching characteristics of the device is a fingerprint of memristive system [26]. Moreover, Chua [27] has claimed that the pinched hysteresis loop can be collapsed into a single-valued function.

Figure 2(a) presents the actual power utilization by the device under test. The power utilized by the device under test is dependent on both applied voltage and current flow through the device. The variation in the current and voltage can lead to a change in the utilized power. The negative direction of power denotes the current direction from ground terminal to excitation terminal. The device utilizes maximum power when the state variable is close to unity, i.e. the device is in the 'ON' state. The modeled data shows  $\sim 2\%$  MED at +4 V as shown in figure 2(a) with respect to the relevant experimental result.





**Figure 2.** (a) Actual power utilization by the device under test. (b) Change in device conductance under negative voltage polarity (sweep rate:  $1.042 \text{ V s}^{-1}$ ). Inset shows the variation in device conductance under positive voltage polarity.



**Figure 3.** (a) Variation in conductance under different voltage amplitude with the pulse number (see the table A in appendix section for applied pulses). (b) Synaptic learning characteristics of memristive system.

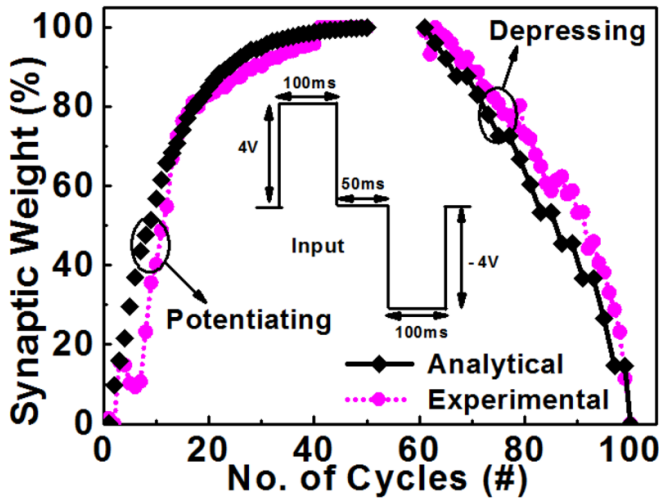
Figure 2(b) displays the change in device conductance under negative voltage bias from 0 to  $-5 \text{ V}$ . However, conductance is a positive quantity, and in this case, the negative direction of conductance under negative voltage polarity denotes the flow of current in the opposite direction and the obtained modeled data shows  $\sim 14.4\%$  MED at  $-2 \text{ V}$  as shown in figure 2(b) with the respective experimental data.

Figure 3(a) shows the change in conductance of the fabricated memristive systems along with their modeled data. Here, it is noted that whenever a chain of 100 successive positive rectangular voltage pulses with different amplitudes (2 V and 2.5 V) and pulse widths (50 ms and 100 ms) are imposed on the memristive system, a significant change in device conductance is observed due to a larger change in the device current [13, 14].

Wang *et al* [28] have also reported similar characteristics for amorphous InGaZnO-based memristive devices. Therefore, if the variation in device conductance is observed as a change in the synaptic weight, then the above discussed mechanism shows closed analogy with the non-linear transmission characteristics of a real biological synapse [26]. The modeled data of device conductance variation under different voltage amplitude shows  $<1\%$  MED with respect to the experimental data.

To investigate the ‘synaptic learning’ behavior of the memristive systems, a chain of 40 successive positive rectangular voltage pulses with an amplitude of 4 V and pulse width of 100 ms is imposed on the device. Under the excitation of such positive successive pulses, the synaptic weight is continuously strengthened along with the number of pulses as the device is continuously in ON state. In this case, the modeled learning behavior shows  $\sim 11.2\%$  MED at pulse number 18, as shown in figure 3(b).

Figure 4 illustrates the synaptic behavior of the memristive system in terms of potentiation and depression processes of learning behavior. Under the application of a chain of 50 successive positive rectangular voltage pulses with an amplitude of  $+4 \text{ V}$  and a pulse width of 100 ms, the synaptic weight of memristive system is continuously strengthened and this mechanism is known as the potentiation. In the case of depression mechanism, a chain of 40 successive negative rectangular voltage pulses with an amplitude of  $-4 \text{ V}$  and a pulse width of 100 ms is applied on the memristive system where the synaptic weight of memristive system is gradually debilitated. After the potentiation and depression mechanisms, the overall electric flux passing through the memristive systems is zero and synaptic weight of the memristive system returns back to its initial stage [4]. This process is similar to the learning behavior of the



**Figure 4.** Change in synaptic weight under the excitation of successive positive (potentiation) and negative (depression) cycles. Inset shows the applied rectangular voltage as an input pulse.

human brain whereas the synaptic weight of the neuromorphic system changes according to the number of electrical stimuli received during the learning process.

The presented analytical model shows  $\sim 4.44\%$  MED at pulse number 85 with respect to the corresponding experimental outcome. The comprehensive advantages of proposed non-linear analytical model are that it has the ability to provide practical outcome for developers and practitioners. Further, the developed analytical memristive model is also applicable for diverse real-time neuromorphic computational applications. This model allows the developer to determine the precision and efficiency of the memristive system. By utilizing the presented analytical modeling, one will be able to investigate the behavior and interactions of the developed memristive system and, therefore, remain better equipped to reduce the complexity of the overall system.

#### 4. Conclusion

Here, a generic non-linear analytical model has been proposed for any material-based memristive system displaying resistive switching, synaptic learning and synaptic plasticity characteristics which are essential parameters for neuromorphic computational applications. The proposed model and its piecewise window function have shown better non-linear behavior in device current at device boundaries by considering the rectifying nature and non-ideal effects which are not incorporated by the other reported models available in the literature. The synaptic plasticity characteristic of modeled data shows  $\sim 4.44\%$  MED in case of  $\text{Y}_2\text{O}_3$  and  $\sim 4.5\%$  MED in case of  $\text{WO}_3$  with respect to corresponding experimental results and these values are the least as compared to values reported in the literature till date. The presented model can be further utilized for the designing and modeling of memristive systems for neuromorphic computation and artificial neural network applications. It is predicted that these properties of the memristive

systems will prove to be helpful for device development to implement hardware for neural network systems.

#### Data availability statement

All data that support the findings of this study are included within the article (and any supplementary files).

#### Acknowledgments

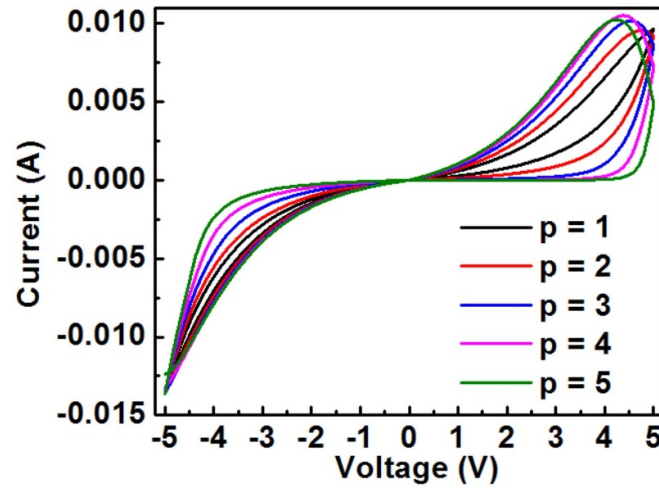
Sanjay Kumar would like to thank DST for providing DST-INSPIRE PhD fellowship. Pawan Kumar would like to thank DST-SERB for providing PhD fellowship. This work is partly supported by CSIR (No. 22(0841)/20/EMR-II).

#### Appendix A

As in equation (2), the value of parameter ' $p$ ' influences the window function which directly affects the  $I$ - $V$  characteristics of the memristive system. The different values of ' $p$ ' change the shape and size of the pinched hysteresis loop in the resistive switching characteristics. In this analytical modeling, we have chosen  $p = 2$  to validate the experimental results and the given range of ' $p$ ' defines the window function between 0 and 1 with the proper shape of  $I$ - $V$  characteristics and obey the necessary conditions as reported by Prodromakis *et al* [21]. Figure A1 displays the impact of the value of parameter ' $p$ ' on the  $I$ - $V$  characteristics of the memristive system. Here, table A shows the applied pulse parameters compute the figure 3(a).

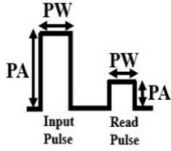
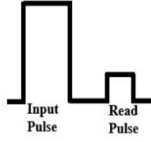
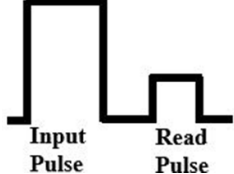
Apart from this the proposed analytical model is also utilized to analyze the performance of  $\text{WO}_3$ -based memristive system for neuromorphic applications. Here, the resistive switching characteristics, utilized actual power, and potentiating and depressing mechanisms for neuromorphic behavior have been discussed. To investigate the various characteristics of  $\text{WO}_3$ -based memristive system, similar electrical conditions are imposed on the memristive systems which have been experimentally reported elsewhere [4]. For the investigation of the resistive switching characteristics of the  $\text{WO}_3$ -based memristive system, a triangular voltage waveform is applied on the device with peak-to-peak voltage of  $\pm 1.3$  V with a compliance current of  $10 \mu\text{A}$ . Figure A2 presents the analytical data along with the reported experimental results of the  $I$ - $V$  characteristics and power utilized by the device under test. Further, analytical data shows  $\sim 31\%$  MED in the  $I$ - $V$  curve and  $\sim 20\%$  MED in utilized power with respect to the experimental data of the device.

Figure A3 illustrates the potentiation ( $P$ ) and depression ( $D$ ) process of the device while studying the synaptic plasticity behavior. During the potentiation process, a chain of 50 successive positive rectangular pulses followed by 50 rectangular negative pulses with an amplitude of  $1.2$  V and pulse width of  $5 \mu\text{s}$  is applied on the device. Under positive pulses, the synaptic weight is strengthened with the number of stimulating positive pulses and debilitated for the negative pulses.



**Figure A1.** Impact of value of parameter ' $p$ ' on resistive switching characteristics of memristive system.

**Table A.** Shape of applied input pulse and read pulse for figure 3(a).

Pulse shape			
			
		For input pulse	
Pulse amplitude (PA)	2 V	2 V	2.5 V
Pulse width (PW)	50 ms	100 ms	100 ms
		For read pulse	
Pulse amplitude (PA)	0.1 V	0.1 V	0.1 V
Pulse width (PW)	10 ms	10 ms	10 ms

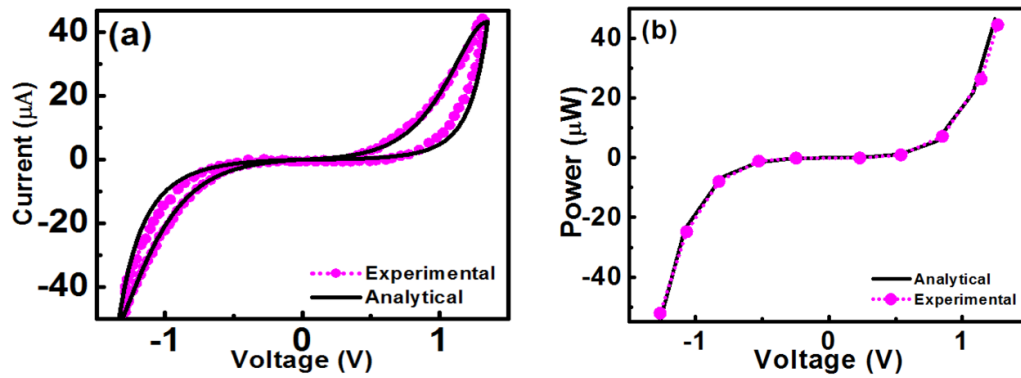


**Figure A2.** (a) Resistive switching characteristics of  $\text{WO}_3$ -based memristive system (sweep rate:  $2 \text{ V s}^{-1}$ ), (b) Actual power utilized by the device under test.

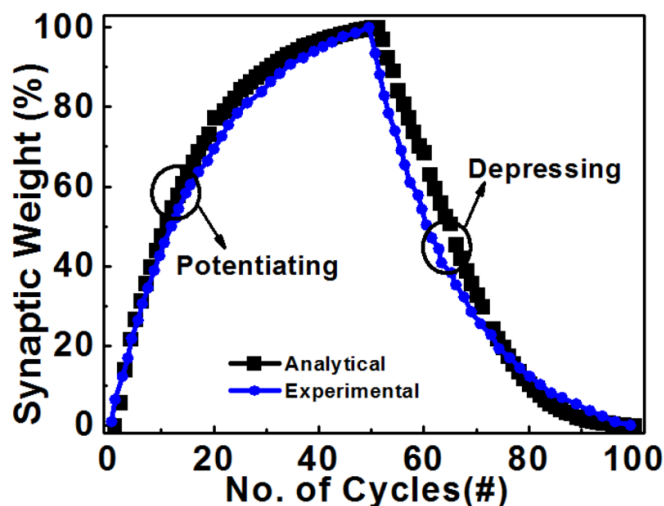


**Figure A3.** Synaptic plasticity behavior of the memristive device under potentiating and depression mechanisms.

Here, the modeled data shows  $\sim 4.5\%$  MED with respect to experimental reported data.

## ORCID iDs

Mangal Das  <https://orcid.org/0000-0001-7596-3133>  
 Shaibal Mukherjee  <https://orcid.org/0000-0002-9879-7278>

## References

- [1] Kuzum D, Yu S and Wong H-S 2013 Synaptic electronics: materials, devices and applications *Nanotechnology* **24** 1–22
- [2] Jeong H and Shi L 2018 Memristor devices for neural networks *J. Phys. D: Appl. Phys.* **52** 1–68
- [3] Li C et al 2018 Analogue signal and image processing with large memristor crossbars *Nat. Electron.* **1** 52–59
- [4] Chang T, Jo S-H, Kim K-H, Sheridan P, Gaba S and Lu W 2011 Synaptic behaviors and modeling of a metal oxide memristive device *Appl. Phys. A* **102** 857–63
- [5] Jo S H, Chang T, Ebong I, Bhadviya B, Mazumder P and Lu W 2010 Nanoscale memristor device as synapse in neuromorphic systems *Nano Lett.* **10** 1297
- [6] Citri A and Malenka R C 2008 Synaptic plasticity: multiple forms, functions, and mechanisms *Neuropsychopharmacol. Rev.* **33** 18–41
- [7] Covi E, Brivio S, Serb A, Prodromakis T, Fanciulli M and Spiga S 2016 HfO<sub>2</sub>-based memristors for neuromorphic applications *IEEE Int. Symp. on Circuits and Systems (ISCAS)* vol 16226481 pp 393–6
- [8] Chang T 2012 Tungsten oxide memristive devices for neuromorphic applications PhD Thesis University of Michigan
- [9] Snider G S 2008 Cortical computing with memristive nanodevices *SciDAC Review* (Winter) pp 58–65
- [10] Jo S H, Kim K-H and Lu W 2009 High-density crossbar arrays based on a Si memristive system *Nano Lett.* **9** 870–4
- [11] Seo K et al 2011 Analog memory and spike-timing-dependent plasticity characteristics of a nanoscale titanium oxide bilayer resistive switching device *Nanotechnology* **22** 1–5
- [12] Kumar A, Das M, Garg V, Sengar B S, Htay M T, Kumar S, Kranti A and Mukherjee S 2017 Forming-free high-endurance Al/ZnO/Al memristor fabricated by dual ion beam sputtering *Appl. Phys. Lett.* **110** 1–5
- [13] Das M, Kumar A, Singh R, Htay M T and Mukherjee S 2018 Realization of synaptic learning and memory functions in Y<sub>2</sub>O<sub>3</sub> based memristive device fabricated by dual ion beam sputtering *Nanotechnology* **29** 1–9
- [14] Das M, Kumar A, Mandal B, Htay M T and Mukherjee S 2018 Impact of Schottky junctions in the transformation of switching modes in amorphous Y<sub>2</sub>O<sub>3</sub>-based memristive system *J. Phys. D: Appl. Phys.* **51** 1–10
- [15] Das M, Kumar A, Kumar S, Mandal B, Siddharth G, Kumar P, Htay M T and Mukherjee S 2020 Impact of interfacial SiO<sub>2</sub> on dual ion beam sputtered Y<sub>2</sub>O<sub>3</sub>-based memristive system *IEEE Trans. Nanotechnol.* **19** 332–7
- [16] Das M, Kumar A, Kumar S, Mandal B, Khan M A and Mukherjee S 2018 Effect of surface variations on the performance of yttria based memristive system *IEEE Electron Device Lett.* **39** 1852–5
- [17] Kvaternik S, Friedman E G, Kolodny A and Weiser U C 2013 TEAM: threshold adaptive memristor model *IEEE Trans. on Circuits and Systems-I Express Brief Regular Paper* vol 60 pp 211–21
- [18] Singh J and Raj B 2019 An accurate and generic window function for nonlinear memristor models *J. Comput. Electron.* **18** 640–7
- [19] Corinto F, Gilli M and Forti M 2018 Flux-charge description of circuits with non-volatile switching memristor devices *IEEE Transactions on Circuits and Systems II: Express Briefs* **65** 642–6
- [20] Kumar S, Agrawal R, Das M, Kumar P and Mukherjee S 2020 Analytical modeling of Y<sub>2</sub>O<sub>3</sub>-based memristive system for synaptic applications *J. Phys. D: Appl. Phys.* **53** 1–6
- [21] Prodromakis T, Peh B P, Papavassiliou C and Toumazou C 2011 A versatile memristor model with nonlinear dopant kinetics *IEEE Trans. Electron Devices* **58** 3099–105
- [22] Yang J J, Pickett M D, Li X, Ohlberg D A A, Stewart D R and Williams R S 2008 Memristive switching mechanism for metal/oxide/metal nanodevices *Nat. Nanotechnol.* **3** 429–33
- [23] Yakopcic C, Taha T M, Subramanyam G, Pino R E and Rogers S 2011 A memristor device model *IEEE Electron Device Lett.* **32** 1436–8
- [24] Bakar R A, Kamarozaman N, Abdullah W F H and Herman S H 2018 Modified hyperbolic sine model for titanium dioxide-based memristive thin films *IOP Conf. Ser.: Mater. Sci. Eng.* **341** 012018
- [25] Hemmati M, Rashtchi V, Maleki A and Toofan S A configurable memristor-based finite impulse response filter (arXiv:1904.05279) pp 1–10
- [26] Chua L and Yang L 1988 Cellular neural networks: theory *IEEE Trans. Circuits Syst.* **35** 1257–72
- [27] Chua L 2011 Resistance switching memories are memristors *Appl. Phys. A* **102** 765–83
- [28] Wang Z Q, Xu H Y, Li X H, Yu H, Liu Y C and Zhu X J 2012 Synaptic learning and memory functions achieved using oxygen ion migration/diffusion in an amorphous InGaZnO memristor *Adv. Funct. Mater.* **22** 2759–65